Neutron Scattering Study of the Normal-Incommensurate Phase Transition in Rb_2ZnBr_4

Hirotake SHIGEMATSU, Hiroyuki MASHIYAMA[1], Masaki TAKESADA[2,*], Ken-ichi OHSHIMA[3], Yasuaki OOHARA[4] and Tsuneo MATSUI

Department of Quantum Engineering, Graduate School of Engineering, Nagoya University, Nagoya 464-8603
[1]*Department of Physics, Faculty of Science, Yamaguchi University, Yamaguchi 753-8512*
[2]*Research Institute for Electronic Science, Hokkaido University, Sapporo 060-0812*
[3]*Institute of Applied Physics, University of Tsukuba, Tsukuba 305-8573*
[4]*Institude for Solid State Physics, University of Tokyo, Roppongi, Tokyo 106-8666*

(Received April 3, 2000)

The soft phonon modes, which are related to the normal-incommensurate phase transition of Rb_2ZnBr_4, have been measured by inelastic neutron scattering. The existence of both phase and amplitude modes has been confirmed, and the phonon dispersion curves have been determined in the low-temperature commensurate phase. On the other hand, the phonon dispersion curve of the transverse acoustic phonon along the (0 0 ξ) direction does not vary appreciably in the normal phase. The soft mode is fully overdamped above the normal-incommensurate phase transition. Diffuse scattering develops around $h0l \pm 5/17$ as temperature approaches T_i = 347 K from above.

KEYWORDS: neutron scattering, phase mode, amplitude mode, normal-incommensurate phase transition, Rb_2ZnBr_4, ferroelectrics

§1. Introduction

Rubidium tetrabromozincate, Rb_2ZnBr_4, belongs to a family of crystals with the β-K_2SO_4 type structure such as Rb_2ZnCl_4.[1,2] The normal phase (phase I) has the orthorhombic structure (space group: $Pmcn$, Z = 4), where the c-axis is a pseudo-hexagonal axis with $b \simeq \sqrt{3}a$. As temperature decreases the crystal transforms to an incommensurate phase (phase II) at T_i = 347 K, where the type of the phase transition is second order one. Hereafter the normal-incommensurate phase transition is abbreviated as the N-INC phase transition. In phase II, the wave vector is represented as q = (1/3-δ)$c_0^* \simeq 5/17c_0^*$, where δ and c_0^* stand for the misfit parameter and the reciprocal-lattice parameter in the normal phase, respectively. The wave vector is almost temperature independent except in the close vicinity of the lock-in transition point (T_C = 187 K).[3] Below T_C, the structure is commensurate with a wave vector of q = $c_0^*/3$. Phase III is ferroelectric along the a-direction (space group: $P2_1cn$, Z = 12, a_0, b_0, $3c_0$), where a_0, b_0 and c_0 are the unit cell parameters in phase I.[1] The crystal has other commensurate phases summarized as followings; phase IV ($112 > T > 76$ K, ferroelectricity//a, antiferroelectricity//b, $2a_0$, $2b_0$, $3c_0$) and phase V ($T < 76$ K, ferroelectricity//a, ferroelectricity//c, $2a_0$, $2b_0$, $3c_0$).[4–6] The space group of phase IV is suggested to be $P11b$ with Z = 24 or twin structure characterized by extra symmetry operations. The space group of phase V is $C1c1$ with Z = 48.[7,8] The melting point of Rb_2ZnBr_4 is reported to be 753 K.[1]

Among the β-K_2SO_4 type ferroelectrics, a soft phonon mode was observed in K_2SeO_4 clearly both above and below the N-INC phase transition point by neutron scattering.[9,10] That is to say, the transition in K_2SeO_4 is interpreted as displacive type one. On the other hand, the soft mode was not observed above N-INC transition point in Rb_2ZnBr_4,[11] Rb_2ZnCl_4[12] and K_2ZnCl_4.[13,14] Therefore it was thought that the transition type was order-disorder one. However, the Raman active modes were observed to soften with approaching to the N-INC transition point from low temperatures.[15–18] According to the phenomenon, it was assumed that a crossover between the displacive and the order-disorder regions occurred.

In the previous paper,[19] we reported the observation of phase and amplitude modes at a Γ point in phase III by neutron scattering. The existence of these modes is indeed quite certain. In the present report, we investigate the observation of the phase mode and the amplitude one with approaching T_i from below, in more detail. The phonon dispersion relation below T_C is presented. A behavior of the Λ_2-Λ_3 transverse branch in the normal phase is determined by inelastic neutron scattering study with the use of hot and cold neutrons. In §2 of this paper, experimental procedures are briefly described. The results of inelastic neutron scattering study are reported in §3 and the N-INC phase transition in Rb_2ZnBr_4 are discussed in the final section.

§2. Experimental

Single crystals of Rb_2ZnBr_4 were grown by slow evaporation method from a saturated aqueous solution of RbBr and $ZnBr_2$ in the molar ratio 1:1 at 308 K.[8] About

* Present address: Kanagawa Academy of Science and Technology, Kawasaki, Kanagawa 213-0012.

three months were needed to grow the single crystals. The obtained crystals were colorless and transparent and showed poor cleavage perpendicularly to the b-axis. Samples were annealed in air at 393 K for ten hours before an experiment to avoid an influence of water contamination.

Triple-axis spectrometers C1-1 and 4G, installed in the guide hall and the reactor hall, respectively, at JRR-3M Reactor of the Japan Atomic Energy Research Institute (JAERI), Tokai, were used for neutron scattering. In the former spectrometer, energy scans were done with a fixed incident neutron beam of $k_{\rm i} = 1.55$ Å^{-1} with a pyrolytic graphite, PG002 monochromator and a PG002 analyzer for requiring a high energy resolution. A beryllium filter was used in order to cut off higher order reflections and the beam collimation of open-open-80'-80' was employed. The full width at half maximum (FWHM) of a Bragg peak was 0.4°. The FWHM of energy transfer for incoherent scattering was 0.2 meV. These conditions were applied for measuring a low-energy excitation below 3 meV. In the latter spectrometer, a fixed incident neutron beam of $k_{\rm i} = 2.57$ Å^{-1} was used for measuring a little more high-angle reflections and high-energy excitation. The used conditions were following: PG002 monochromator, PG002 analyzer, PG filter and 40'-40'-40'-40' collimation. Under such conditions the FWHM of energy transfer for incoherent scattering was about 1 meV.

In both spectrometers, a crystal with a size of about 13 cm^3 was mounted in an aluminum can filled with helium gas and set in a closed-cycle refrigerator which was cooled by cryogenics below room temperature or in an electric furnace above room temperature. The sample temperature was controlled within 0.1 K by a TEMCON-IV system developed by Prof. Y. Noda of Tohoku University. The data collections were carried out in the (a^*, c^*) scattering plane and the measurements of phonon dispersion were performed along the line 200-202 for C1-1 and the lines 200-202 and 400-402 for 4G. Lattice parameters were determined from the two reflections 400 and 002: $a_0 = 7.63$ Å and $c_0 = 9.64$ Å at 250 K.

§3. Results

Figure 1 shows the results of energy scan with constant Q at $20\frac{22}{17}$ (at 210 K) and at $20\frac{4}{3}$ (below $T_{\rm C}$) by the use of C1-1. The quasi-elastic scattering can be fitted by the relation $I = I_{\rm B} + a\exp(-E^2/b) + c/(d + E^2 + fE^4)$,[19] which is shown by the solid line. Here E is the energy transfer, $I_{\rm B}$ is the background and a, b, c, d and f are parameters, which are determined to fit the central part of quasi-elastic scattering (not shown in Fig. 1 explicitly). The energy scans at the position of the satellite exhibit a central peak in addition to the inelastic response from the soft mode.

Since a temperature independent Raman active mode has been observed at 25 cm^{-1} (about 3.1 meV),[15,16] the increase in signal below -2.7 meV was interpreted to be influenced by the Raman mode. Therefore, the observed phonon peaks except for the quasi-elastic scattering were fitted to three Lorentzian-type cross sections (phase, amplitude and 3.1 meV modes) convoluted with the instrumental resolution function. The excitation peaks of the phase and the amplitude modes are indicated by arrows at 80 K in Fig. 1. Although the observed peaks are weak, these two peaks are recognized as the phase and the amplitude modes in the low-temperature commensurate phases.

On the other hand, in the incommensurate phase, the presence of these modes have not been clearly confirmed , because the phase mode has been influenced by an incoherent scattering and the amplitude mode has become so broad. Furthermore, the splitting of the phase mode spectrum into an acoustic-like and an optic-like branch could not been observed in the second-order satellite point.[20,21]

The phonon dispersion curves are shown in Fig. 2 in an extended zone scheme along the (0 0 ξ) direction at 70 K, 20ξ: $0 \le \xi \le \frac{1}{3}$, 202-$\xi$: $\frac{1}{3} \le \xi \le \frac{2}{3}$ and 20ξ: $\frac{2}{3} \le \xi \le 1$, by the use of C1-1.[10] In the vicinity of $\xi = \frac{2}{3}$, TA branches are observed clearly because the $\xi = \frac{2}{3}$ point becomes equivalent to the Γ point, and the reflections $20\frac{2}{3}$ and $20\frac{4}{3}$ become strong superlattice reflections below $T_{\rm C}$. Although it is expected that the dispersion curves in the periodic zone scheme should be periodic,[10] some parts of branches was so broad and weak that it was difficult to observe the whole branches. In Fig. 2, the clearly observed peaks are plotted.

Figure 3 shows the temperature dependence of phase and amplitude mode energies observed at $20\frac{4}{3}$ below $T_{\rm i}$. Full circles and full triangles are neutron data points for the amplitude and the phase mode, respectively. Furthermore, open circles and open triangles show the Raman spectra for $c(aa)b$ and $c(ac)b$ geometries given in ref. 15, respectively. The obtained data coincide well with each other. This result indicates that the phase and the amplitude modes are underdamped at least in the low-temperature region. Furthermore, it should be noted that no changes were recognized in these phonon modes either at the phase III-to-IV transition or at the phase IV-to-V transition.

Figure 4 shows the energy scan spectrum with constant Q at 510 K, a typical spectrum in the normal phase. For low Q (Q = 20ξ: $\xi = 0.2$ and 0.4), the spectrum was observed by the use of C1-1 with high resolution but weak intensity. On the other hand, the 4G spectrometer was used for high Q (Q = 40ξ: $\xi = 0.6, 0.8$ and 1.0). The observed peak was recognized as a transverse acoustic (TA) phonon. The incoherent scattering can be observed at low energy transfer less than 1 meV, which exhibited weak Q dependence except for around Γ points. The dispersion branch of the TA mode is summarized in Fig. 5. With increasing temperature, the slope of the branch decreases a little indicating the decrease of the elastic constant as the crystal approaches the melting point.

Although the TA phonon was clearly observed, no softening of the branch was observed around $\xi = \frac{2}{3}$ ($20\frac{2}{3}$, $20\frac{4}{3}$, $40\frac{2}{3}$ or $40\frac{4}{3}$), where the softening was reported in the case of K_2SeO_4.[9] Instead of such soft phonon, we measured quasi-elastic diffuse scattering around the points of $\xi = \frac{2}{3}$ in the normal phase.[22] Figure 6 shows the results of energy scan with constant Q at $20\frac{22}{17}$ above $T_{\rm i}$, by the use of C1-1. We could not measure an en-

ergy excitation above 2.4 meV because of a restriction of the instrument. The quasi-elastic intensity rapidly grows with approaching the transition temperature. The width of the excitation seems to be less than the instrumental resolution.

Figure 7 shows the temperature dependence of the diffuse scattering intensities at the $20\frac{22}{17}$-0.04, $20\frac{22}{17}$-0.035 and $20\frac{22}{17}$ points and the temperature dependence of the inverse intensity, corrected for the background, at the $20\frac{22}{17}$ point by the use of 4G. Above the transition temperature $T_{\rm i}$, the inverse intensity varies almost linearly with temperature and tends to zero at 343 K, which corresponds to the temperature of maximum intensity at the $20\frac{22}{17}$-0.04 and $20\frac{22}{17}$-0.035,[1] and it is considered $T_{\rm i}$ of our crystal.

§4. Discussion

The phase and the amplitude modes were observed in the low-temperature phases by the inelastic neutron scattering. In addition, the phonon dispersion curves, which were almost the same as K_2SeO_4,[10] were confirmed at 70 K, although the mode frequencies in Rb_2ZnBr_4 were lower than those in K_2SeO_4. In the low-temperature phases III, IV and V, the dispersion curve with TA branch is shown as the trisection of the zone, which is folded back of the dispersion (Fig. 5) along the lines $\xi = \frac{1}{3}$ and $\frac{2}{3}$.[13] Therefore, we can obtain excitation peak around 3.2 meV on a Γ point. This excitation peak corresponds to the 25 $\rm cm^{-1}$ $c(aa)b$ Raman active mode. The hump below -2.7 meV in Fig. 1 is considered to be the wing of the mode.

The phase mode is generally overdamped in incommensurate phase because the mode frequency is very low. On the contrary, the damping vanishes as the frequency for the case of acoustic phonon. This is considered why the phase mode has not been observed in many crystal systems. The theory of incommensurate systems predicts the existence of a gapless acoustic-like phase mode branch in addition to the optic-like amplitude mode branch.[21] In this study, the possible existence or non-existence of an energy gap in the phase mode excitation could not been determined in the normal phase.

Although the amplitude and phase modes, which make a contribution to the N-INC phase transition, are clearly observable in the low-temperature commensurate phase, the soft mode seems to be fully overdamped above $T_{\rm i}$. This observation supports the results studied by many authors.[7,8,13,18,19] Therefore, the N-INC phase transition in Rb_2ZnBr_4 is considered to be neither a simple order-disorder type nor a simple displacive type. The mechanism responsible for the N-INC phase transition in Rb_2ZnBr_4 is similar to that in Rb_2ZnCl_4 and K_2ZnCl_4.

Samara pointed out an empirical rule between the pressure coefficient $\mathrm{d}T/\mathrm{d}p$ of the transition temperature and the mechanisms of the phase transition: (1) A displacive type transition, in which an optical phonon freezes at zone-boundary, has the positive pressure coefficient $\mathrm{d}T/\mathrm{d}p$, (2) a ferroelectric transition is a displacive type, in which an optical phonon freezes at zone-center, and has the pressure coefficient is negative, (3) if an order-disorder type mode freezes at zone-center, then the pressure coefficient is positive.[23,24] The Samara's rule is effective as a means of getting information about the transition mechanism. In many β-K_2SO_4 type ferroelectrics, the type of a second ferroelectric phase transition (phase III-to-IV transition) can be explained quite naturally by the item (1) of the Samara's rule: The underdamped soft modes were observed at the zone-boundary S point and positive pressure coefficient $\mathrm{d}T_{\rm III-IV}/\mathrm{d}p = 70$ K/GPa for Rb_2ZnBr_4, 68 K/GPa for K_2ZnCl_4 and 84 K/GPa for K_2CoCl_4.[8,14,25,26]

Furthermore, in the N-INC phase transition, Gesi discussed the relation between the N-INC phase transition temperature $T_{\rm i}$ and the pressure coefficient for various β-K_2SO_4 type ferroelectrics as a good example of an application of Samara's rule.[27] Gesi found that the N-INC transition is displacive if $T_{\rm i}$ is very low and the pressure coefficient is negative. On the other hand, as $T_{\rm i}$ becomes high, the pressure coefficient changes from negative to positive, and the transition mechanism is rather order-disorder type. Therefore he proposed that the magnitude of $T_{\rm i}$ is correlated both to $\mathrm{d}T_{\rm i}/\mathrm{d}p$ and to the transition mechanism. An underdamped soft mode was observed in K_2SeO_4, which has the lowest $T_{\rm i}$ and negative pressure coefficient (-65.5, -65 or -73 K/GPa).[28–30] Furthermore, the soft modes in K_2SeO_4 showed strong hardening below $T_{\rm i}$ and the scattering intensity of the soft mode increased rapidly with decreasing temperature.[31] On the other hand, in Rb_2ZnBr_4 (58 K/GPa), Rb_2ZnCl_4 (3.5 K/GPa) and K_2ZnCl_4 (110 K/GPa), which have positive coefficients,[32,33] well-defined soft modes have not been observed in the normal phase.[15–17] The soft modes showed weak hardening far below $T_{\rm i}$. The order-disorder nature becomes remarkable as the transition temperature $T_{\rm i}$ increases, which has been considered to be related to the librational motion of the tetrahedron.[22]

In Rb_2CoCl_4, although the absolute value of the pressure coefficient is small, the coefficient is negative (-12 K/GPa).[27] Therefore, we expect that the underdamped soft modes will be observable in the normal phase. Incidentally, two low-energy modes, which were fairly dependent on temperature, were observed below $T_{\rm i}$ by light scattering.[34] The inelastic neutron scattering study on Rb_2CoCl_4 is now in progress.

1) S. Sawada, Y. Shiroishi, A. Yamamoto, M. Takashige and M. Matsuo: J. Phys. Soc. Jpn. **43** (1977) 2101.
2) C. J. de Pater and C. van Dijk: Phys. Rev. B **18** (1978) 1281.
3) K. Gesi and M. Iizumi: J. Phys. Soc. Jpn. **45** (1978) 1777.
4) T. Ueda, S. Iida and H. Terauchi: J. Phys. Soc. Jpn. **51** (1982) 3953.
5) H. Kasano, H. Shigematsu, H. Mashiyama, Y. Iwata, H. Kasatani and H. Terauchi: J. Phys. Soc. Jpn. **63** (1994) 1681.
6) T. Yamaguchi and S. Sawada: J. Phys. Soc. Jpn. **60** (1991) 3162.
7) H. Shigematsu, H. Mashiyama, Y. Oohara and K. Ohshima:

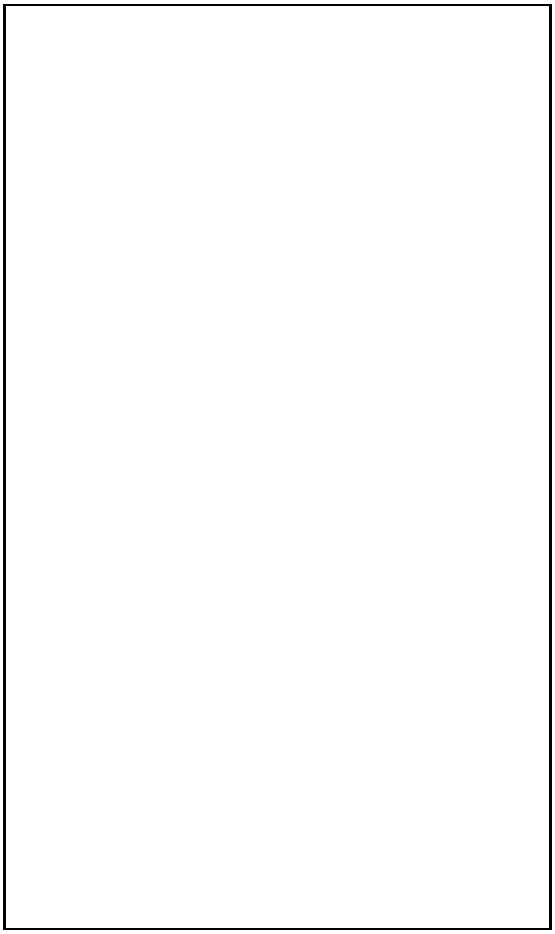

Fig. 1. Neutron scattering spectrum at $20\frac{22}{17}$ (at 210 K) and at $20\frac{4}{3}$ (at 180, 150, 120 and 80 K). Two modes, which are indicated by arrows, are resolved below $T_C = 187$ K: the lower-frequency peak is the phase mode, and the upper one is the amplitude mode.

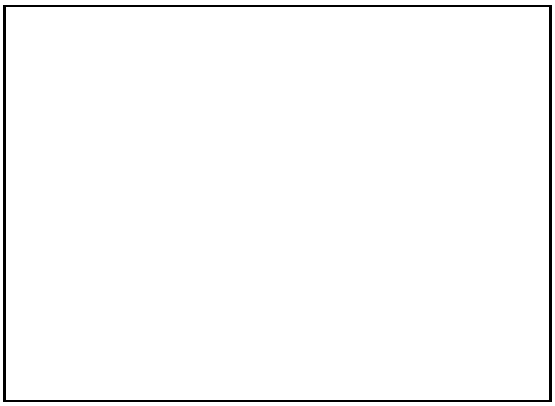

Fig. 2. Phonon dispersion curves in an extended-zone scheme on the (0 0 ξ) line at 70 K. Solid and broken lines are just a guide to the eye.

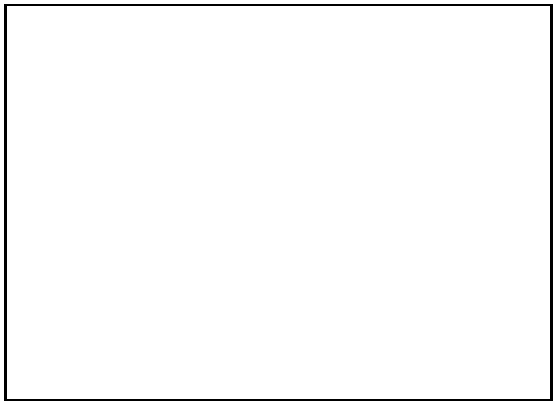

Fig. 3. Temperature dependence of phase and amplitude mode frequencies at $20\frac{4}{3}$ below T_i. Full circles and full triangles are neutron data point for the amplitude and the phase modes, respectively. Open circles and open triangles show the Raman spectra for $c(aa)b$ and $c(ac)b$ geometries in ref. 15, respectively. Solid and broken lines are just a guide to the eye.

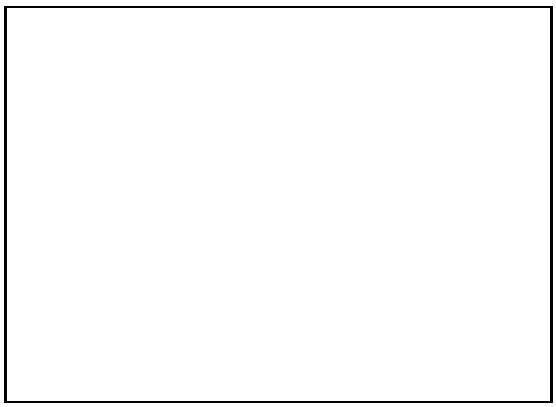

Fig. 4. Neutron scattering spectrum (energy scan with constant Q) at 510 K. The spectra for $\xi = 0.2$ and 0.4 were measured by the use of C1-1, while those for $\xi = 0.6$, 0.8 and 1.0 were by use of the 4G under low resolution but high intensity.

Physica B **219&220** (1996) 611.

8) H. Shigematsu, H. Mashiyama, Y. Oohara and K. Ohshima: J. Phys. :Condensed Matter **10** (1998) 5861.
9) M. Iizumi, J. D. Axe, G. Shirane: Phys. Rev. B **15** (1977) 4392.
10) J. D. Axe, M. Iizumi and G. Shirane and K. Shimaoka: Phys. Rev. B **22** (1980) 3408.
11) C. J. de Pater, J. D. Axe and R. Currat: Phys. Rev. B **19** (1979) 4684.
12) H. Mashiyama, H. Shigematsu, K. Sugimoto, H. Kawano, Y. Oohara and H. Yoshizawa: J. Korean Phys. Soc. (Proc. Suppl.) **27** (1994) S98.
13) K. Gesi and M. Iizumi: J. Phys. Soc. Jpn. **53** (1984) 4271.
14) M. Quilichini, V. Dvorak and P. Boutrouille: J. Phys. I. France **1** (1991) 1321.
15) E. Francke, M. Le Postollec, J. P. Mathieu and H. Poulet: Solid State Commun. **35** (1980) 183.
16) M. Takashige, T. Nakamura, M. Udagawa, S. Kojima, S. Hirotsu and S. Sawada: J. Phys. Soc. Jpn. **48** (1980) 150.
17) M. Wada, A. Sawada and Y. Ishibashi: J. Phys. Soc. Jpn. **50**

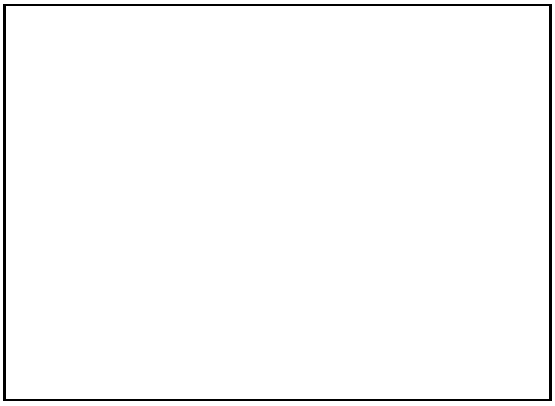

Fig. 5. Phonon dispersion curves along the (0 0 ξ) direction at 300, 450, 510 and 600 K in the normal phase of Rb_2ZnBr_4.

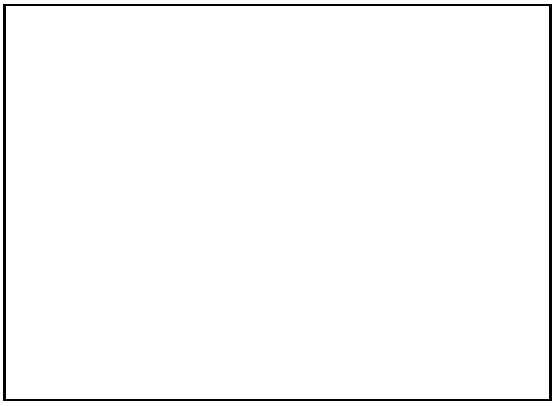

Fig. 7. The temperature dependence of the diffuse scattering intensities at the $20\frac{22}{17}$-0.04 ($\diamond$), $20\frac{22}{17}$-0.035 ($\triangle$) and $20\frac{22}{17}$ ($\circ$) points in Rb_2ZnBr_4. The inverse intensity, corrected for the background, at the $20\frac{22}{17}$ is drawn by closed circles ($\bullet$).

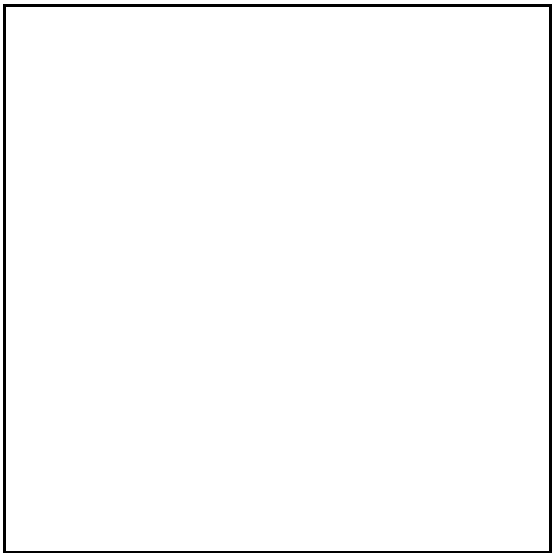

Fig. 6. Neutron scattering spectrum in the normal phase ($T > T_i = 347$ K) at Q = $20\frac{22}{17}$, indicating the remarkable increase of the quasi-elastic scattering with approaching T_i.

(1981) 531.

18) T. Sekine, M. Takayama, K. Uchinokura and E. Matsuura: J. Phys. Soc. Jpn. **55** (1986) 3903.
19) H. Mashiyama, H. Shigematsu and Y. Oohara: Physica B **213**&**214** (1995) 439.
20) M. Quilichini and R. Currat: Solid State Commun. **48** (1983) 1011.
21) R. Blinc, P. Prelovsek, V. Rutar, J. Seliger and S. Zumer: *Incommensurate Phases in Dielectrics*, ed. R. Blinc and A. P. Levanyuk (North-Nolland, 1986, Amsterdam) Chap. 4.
22) H. Mashiyama: J. Korean Phys. Soc. (Proc. Suppl.) **29** (1996) S419.
23) G. A. Samara: J. Phys. Soc. Jpn. **28** (1970) Suppl. 399.
24) G. A. Samara, T. Sakudo and K. Yoshimitsu: Phys. Rev. Lett. **29** (1975) 1767.
25) I. N. Flerov, T. Yamaguchi, S. Sawada, M. V. Gorev and K. S. Aleksandrov: J. Phys. Soc. Jpn. **61** (1992) 1606.
26) H. Shigematsu, M. Kubota, M. Nishi, H. Mashiyama and T. Matsui: J. Phys. Soc. Jpn. **68** (1999) 2679.
27) K. Gesi: J. Phys. Soc. Jpn. **59** (1990) 1841.
28) G. A. Samara: Ferroelectrics **36** (1981) 335.
29) W. Press, C. F. Majkrzak, J. D. Axe, J. R. Hardy, N. E. Massa and F. G. Ullman: Phys. Rev. B **22** (1980) 332.
30) S. Kudo and T. Ikeda: J. Phys. Soc. Jpn. **50** (1981) 733.
31) M. Wada, H. Uwe, A. Sawada, Y. Ishibashi, Y. Takagi and T. Sakudo: J. Phys. Soc. Jpn. **43** (1977) 544.
32) K. Gesi: Ferroelectrics **64** (1985) 97.
33) K. Gesi: J. Phys. Soc. Jpn. **53** (1984) 62.
34) V. I. Torgashev, Yu. I. Yuzyuk, F. Smutny, P. Vanek and B. Brezina: Phys. Status Solidi B **154** (1989) 777.

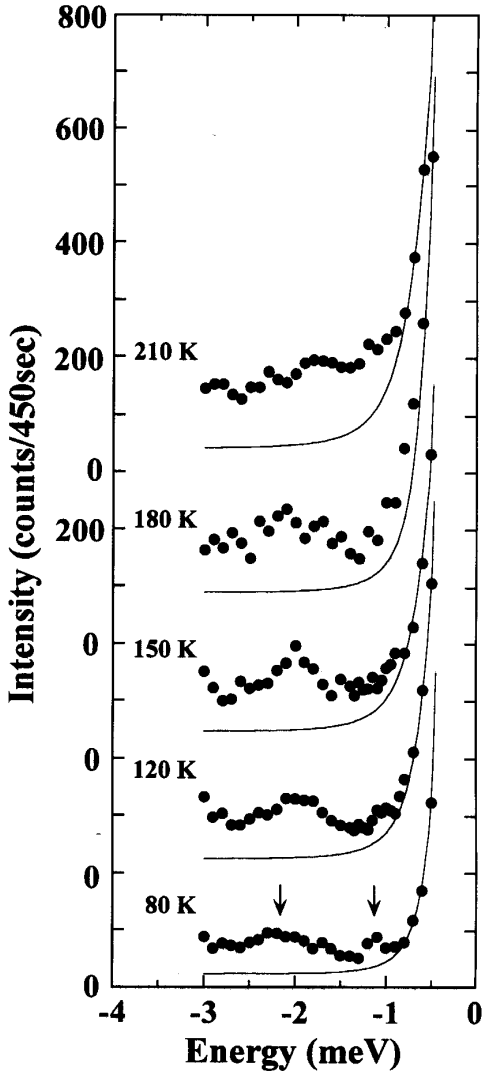
800
600
400
200
0
200
0
0
0
0
210 K
180 K
150 K
120 K
80 K
Intensity (counts/450sec)
-4
-3
-2
-1
0
Energy (meV)

Fig. 1.

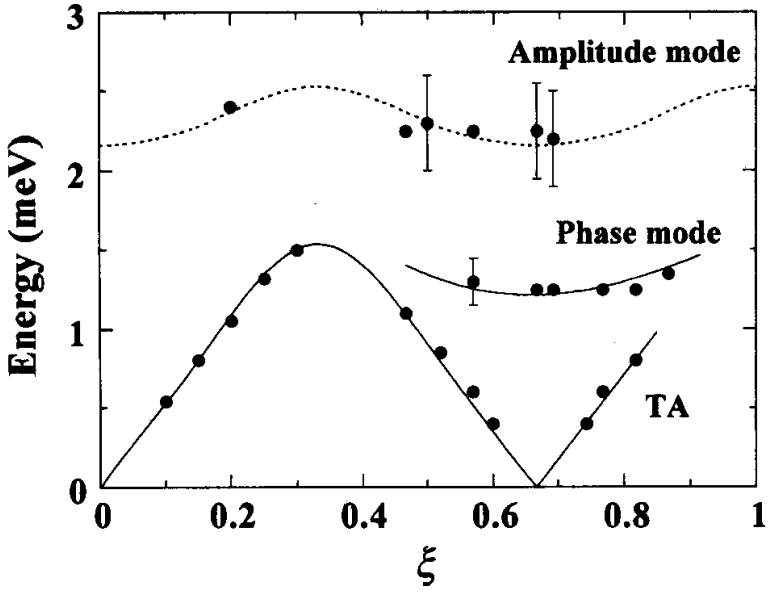
3
2
1
0
Amplitude mode
Phase mode
TA
Energy (meV)
0
0.2
0.4
0.6
0.8
1
ξ

Fig. 2.

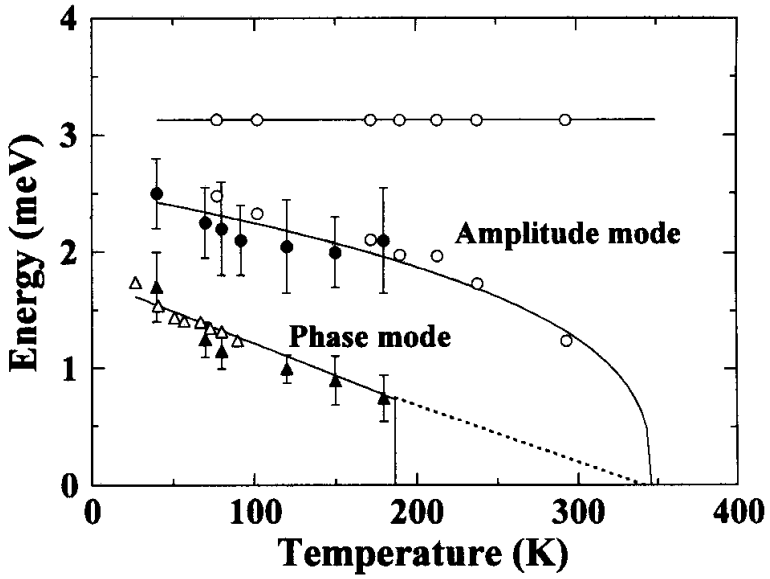
Energy (meV)
Temperature (K)
Amplitude mode
Phase mode
0
1
2
3
4
0
100
200
300
400

Fig. 4.

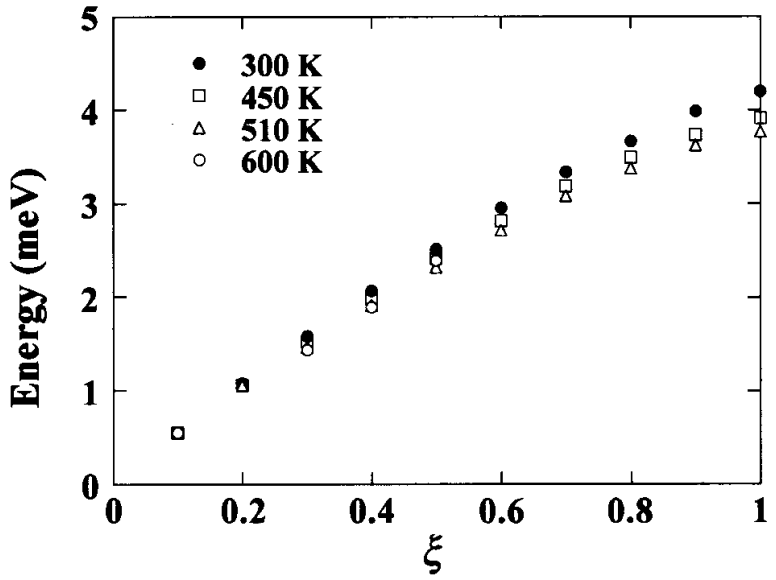
Energy (meV)
ξ
300 K
450 K
510 K
600 K
0
1
2
3
4
5
0
0.2
0.4
0.6
0.8
1

Fig. 5.

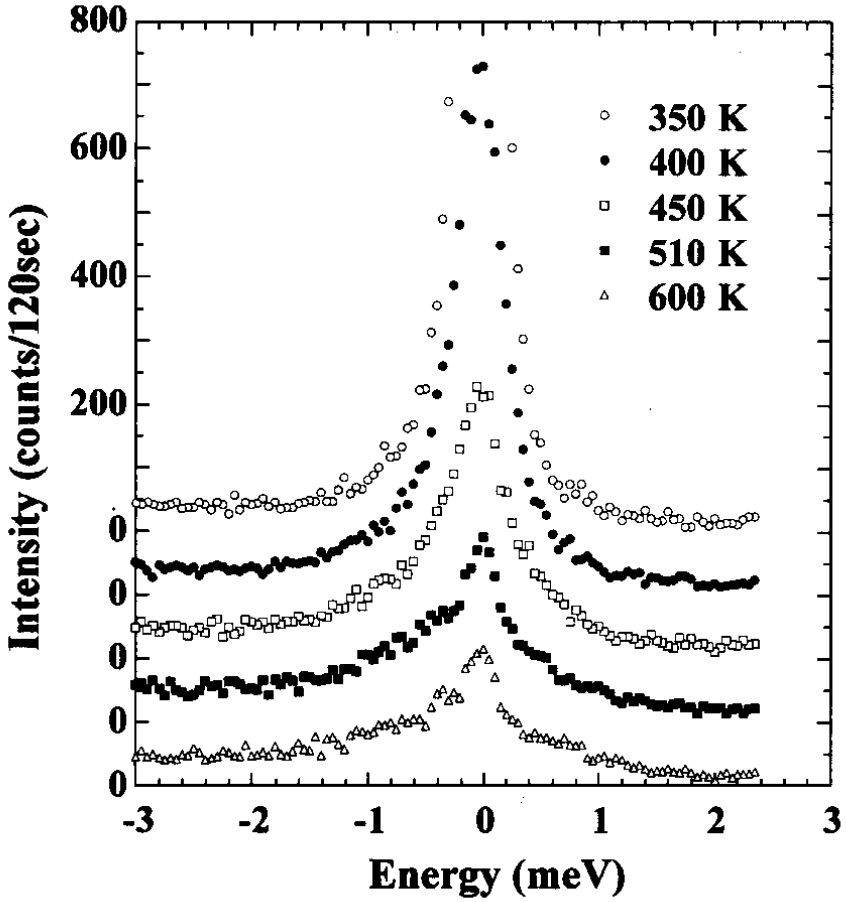
800
600
400
200
0
0
0
0
0
-3
-2
-1
0
1
2
3
Intensity (counts/120sec)
Energy (meV)
350 K
400 K
450 K
510 K
600 K

Fig. 6

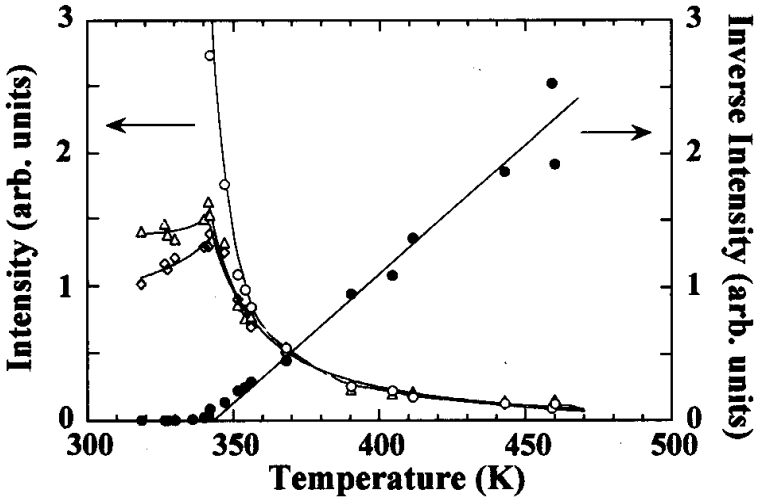
3
2
1
0
300
350
400
450
500
Intensity (arb. units)
Inverse Intensity (arb. units)
Temperature (K)

Fig. 7.